SLOVAK UNIVERSITY OF TECHNOLOGY IN BRATISLAVA
FACULTY OF CIVIL ENGINEERING

Ing. Adam Novák

Dissertation Thesis Abstract

Investigation of hydrological signal in repeated and stationary gravity measurements

to obtain the Academic Title of Philosophiae Doctor (PhD.)

In the doctorate degree study programme:

3636 Geodesy and Cartography

Form of study:

Full-time study

Bratislava 2023

Dissertation Thesis has been prepared at the Department of theoretical geodesy and geoinformatics, Faculty of Civil Engineering, Slovak University of Technology in Bratislava.

Submitter: Ing. Adam Novák
Department of theoretical geodesy and geoinformatics
Faculty of Civil Engineering, STU in Bratislava
Radlinského 11, 810 05 Bratislava

Supervisor: prof. Ing. Juraj Janák, PhD.
Department of theoretical geodesy and geoinformatics
Faculty of Civil Engineering, STU in Bratislava
Radlinského 11, 810 05 Bratislava

Reviewers: doc. Ing. Michal Šprlák, PhD.
Department of Geomatics
University of West Bohemia, Faculty of Applied Sciences
Technická 8, 306 14 Plzeň, Czech republic

prof. Ing. Kostelecký Jan, DrSc.
Department of Geodesy and Surveying
Technical University of Ostrava, Faculty of Mining and Geology
17. listopadu 2172/15. 708 00 Ostrava-Poruba

Ing. Michal Mikolaj, PhD.
DEUTSCHE TELEKOM SERVICES EUROPE CZECH REPUBLIC
Holandská 859/3, 639 00 Brno

Dissertation Thesis Abstract was sent : ....

Dissertation Thesis Defence will be held on............................. **at** ....

at Department of theoretical geodesy and geoinformatics, Faculty of Civil Engineering STU in Bratislava, Radlinského 11, 810 05 Bratislava.

prof. Ing. Stanislav Unčík, PhD.
Dean of Faculty of Civil Engineering

Abstract

The submitted work provides an overview of the methods that are commonly used to reduce the influence of the redistribution of water masses on gravity measurements. Due to the magnitude of the gravity signal it produces, hydrology is considered one of the most important phenomena contributing to time-varying gravity. In this work, we describe a methodology that can be used to reduce the influence of hydrology on gravity measurements in three consecutive steps. First, data from global hydrological models are used to calculate the gravitational effect of distant water masses and their loading effect. Secondly, the gravitational effect of groundwater level variations in the vicinity of the instrument is taken into account. The last component covers the influence of water mass redistribution in the unsaturated zone. We have developed a tool that allows the calculation of the soil moisture effect by forcing different meteorological and hydrogeological data into a single hydrological model. The proposed method has been tested on data from a variety of gravimeters to demonstrate its effectiveness. The results show a reduction in residual gravity variations of up to 70%.

Key words:

Gravimetry
Stationary gravity measurements
Hydrological signal
Global hydrological cycle

Abstrakt

Predložená práca poskytuje prehľad metód, bežne využívaných na zníženie vplyvu hydrológie na merania tiažového zrýchlenia. Vzhľadom na veľkosť gravitačného signálu, ktorý produkujú presun hydrologických hmôt, sa hydrológia považuje za jeden z najdôležitejších javov, ktoré prispievajú k zmenám tiažového zrýchlenia. V práci je opísaná metodika, ktorú možno použiť na zníženie vplyvu hydrológie na gravimetrické merania v troch po sebe nasledujúcich krokoch. Na výpočet gravitačného účinku vzdialených vodných más a ich deformačného účinku sú využité údaje z globálnych hydrologických modelov. Druhá zložka zohľadňuje gravitačný účinok zmien hladiny podzemnej vody v blízkosti prístroja. Posledná zložka zahŕňa vplyv zmien množstva hydrologických hmôt v nenasýtenej pôdnej vrstve. V práci je zároveň predstavený nástroj, ktorý umožňuje výpočet vplyvu pôdnej vlhkosti kombináciou rôznych meteorologických a hydrogeologických údajov do jedného hydrologického modelu. Účinnosť navrhovanej metódy bola testovaná na údajoch z rôznych gravimetrov s cieľom znížiť vplyv hydrológie. Použitie uvedeného postupu redukuje variáciu tiažového zrýchlenia až o 70%.

Kľúčové slová

Gravimetria
Staničné merania tiažového zrýchlenia
Hydrologický signál
Globálny hydrologický cyklus

Introduction

Gravimetry is a science that measures the strength of a gravitational field. It is mainly used to study the Earth's gravitational field and its variations, but it can also be applied to other celestial bodies and objects with a gravitational field. Recent advances in technology have led to the development of new and improved instruments and measurement techniques that have been used to map gravity field with unprecedent accuracy. For example, the Gravity Recovery and Climate Experiment (GRACE) satellite mission (JPL – NASA, online) and its successor GRACE - Follow On (GRACE - FO), enabled the study of Earth's gravity field variations on a global scale.

In addition to satellite gravimetry, there are also airborne (Jekeli, 1994) and ground-based gravimeters which are more suitable for study of local gravity field variations. Both airborne and terrestrial gravimetry can be applied in various fields such as the mineral exploration, environmental monitoring or establishment of reference frames. It allows the mapping of subsurface structures that may indicate the presence of deposits. In environmental monitoring, it is used to detect changes in the Earth's gravity field caused by mass redistributions over time (Van Camp et al., 2017).

The two main instrument types used in terrestrial gravity measurements are absolute and relative gravimeters. The most common type of the absolute gravimeter – a ballistic gravimeter measures the gravity by observing the motion of a free-falling mass. The basic principle of the ballistic gravimeter is to release a test mass from a fixed height and measure its position as it falls. Its acceleration due to gravity can then be calculated from the measured position and time (Faller, 1965; Palinkas and Kostelecky, 2012). Absolute gravimeters are typically used to establish and maintain national reference frames or for calibration of relative instruments. Other than that, their use is limited due to a relatively complicated transportation and expensive maintenance. Relative gravimeters on the other hand have a limited range and are only able to measure the variations within the local gravity field. They can be used for terrain measurements as they are much more compact, easier to manufacture and transfer between observed points than absolute gravimeters (Fores et al., 2019).

For two decades, hydrology has remained among the most studied environmental phenomenon, regarding the use of stationary gravity measurements. This statement is supported by two main reasons. When using gravity measurements to analyze other, non-hydrology related effects, we first need to remove as much hydrological signal as possible. Otherwise, the presence of hydrological signal can significantly change the interpretation of results. Depending on the location, the scale of the hydrological signal present in gravity data can vary from few $nm.s^{-2}$ to hundredths of $nm.s^{-2}$ (Lampitelli and Francis, 2010). An extreme example of the hydrological effect is a 400 $m.s^{-2}$ difference between gravity measurements performed in winter and summer months at the Zugspitze gravimetric base points in German Alps (Flury et al., 2006). The use of hydrological correction gains importance with the requirement for increased sensitivity of the gravimeter to weaker gravity signals. These can often be overshadowed by the presence of hydrology in the recordings, reducing the signal-to-noise ratio (SNR) of the phenomenon being studied. Numerous studies e.g. (Lampitelli and Francis, 2010; Meurers, 2006) have shown the importance of correcting gravity series for the influence of hydrology. Nevertheless, correcting gravity observations for the influence of hydrology remains challenging due to the amount of data and time required and missing conventions.

At the same time, gravity measurements are increasingly being used to monitor local variations in water storage. When used correctly, they provide a potential means of calibrating hydrological models (Christiansen et al., 2009). The integral nature of the gravity measurements means that they provide unique information about all the hydrological masses in the vicinity, unlike other hydrological instruments, unlike other hydrological instruments which tend to specialise in one particular parameter. In this paper we provide an overview of methods commonly used to correct gravity measurements for the influence of water mass redistribution. For the reasons provided later, the hydrological effect calculation is split into two parts, global and local component. Since the local hydrological effect is more challenging, we have developed a tool for it's estimation. To assess the effectiveness of computed hydrological effect, we use data from both relative and absolute gravimeters.

The work is structured into introduction and 5 numbered sections. Sections 1 and 2 describe the current status of the problems analysed and the theoretical background. Section 1 provides an overview of instruments currently used in terrestrial gravity measurements and measuring techniques involved. Special attention is paid to a describing correction procedure required to obtain residual gravity series suitable for hydrological analyses. The second section describes methods for monitoring water mass redistribution at both local and global scale, and previous work involving hydrological analyses based on gravity measurements. The third section provides a 3-step procedure for calculating the hydrological correction and a tool we have developed for this purpose. To validate the proposed methodology and show its effectiveness, we compare the modelled hydrological effect with data from various gravity measurements. Section 4 provides assessment of the results with respect to aims and objectives set during the dissertation exam and section 5 gives general conclusions.

1 Gravity measurements

In 1687 Sir Isaac Newton published his work ''Philosophiæ Naturalis Principia Mathematica'' (Mathematical Principles of Natural Philosophy) with three laws of motion and a fundamental gravitational law, which describes the interaction between two objects (1.1).

$$F_g = G\frac{m_1 m_2}{d^2} \tag{1.1}$$

In its scalar form the absolute value of gravitational force vector F_g of two mutually attracted bodies is calculated based on their masses m_1 and m_2 , distance *d* and the gravitational constant *G* (Janak, 2010; Heiskanen and Moritz, 1967). Newton's work had contributed to the development of the theory of gravity, but also triggered further discussions about the shape of the Earth. His work was followed in 1743 by A.C. Clairaut's "Théorie de la Figure de la Terre", which contained a theorem relating the geometric flattening of the Earth to the difference between the equatorial and polar gravitational forces. A further idea was proposed by J. F. C. Gauss that the shape of the Earth should reflect its internal distribution as seen by the gravitational field, rather than relying solely on geometric measurements of the Earth's surface. Since then, measurements of the gravitational field have been used to define the shape of the Earth (Torge, 1989).

Absolute gravimeters

Absolute gravimeter (AG) is a device capable of determining the absolute value of gravity vector g ($g = |\vec{g}|$). Technological progress in 20th century related to time measurement accuracy (quartz clock development) allowed first tests of direct free-fall (Volet, 1946) and symmetrical rise and fall method (Cook, 1967) in gravity measurements. Since then absolute gravity measurements have been carried out almost exclusively using free-fall method. A major improvement of absolute ballistic gravimeters was introduced with the use of a laser interferometer able to continuously keep track of free-falling object (Hammond and Faller, 1967). Additional improvements such as use of super-spring have increased the accuracy and repeatability to few µGal (10^{-8}m.s^{-2}). The FG5X and its predecessor the FG5, manufactured by Micro-g solutions (https://microglacoste.com/), are currently the most widely used commercial absolute gravimeters. Numerous tests have shown, that the repeatability of gravity measurements performed by these instruments is better than 16 nm.s^{-2} (Van Camp et al., 2005). Both instruments use rubidium clock with accuracy of 10^{-12} s as a time reference. Interferometric measurement of distance as a function of time is provided by a Helium-Neon laser with frequency stabilized by iodide vapor (Janak, 2010). Along with the gravimeter, the company also supplies the g9 software used for data acquisition and processing. During the free fall of a test mass in vacuum chamber, more than 1 million couples of measured distance and time are recorded. Using the least square adjustment (LSA), on the equation (1.1) describing non-homogenous gravity field where we assume constant vertical gravity gradient W_{zz}, we estimate the so-called acceleration of free fall at the top of the chamber g_0 (Timmen, 2010). This value however is time dependent and requires use of several reductions related to measuring process and gravity changes in time.

$$z(t) = z_0\left(1+\frac{1}{2}W_{zz}\tilde{t}^2\right) + v_0\tilde{t}\left(1+\frac{1}{6}W_{zz}\tilde{t}^2\right) + \frac{1}{2}g_0\tilde{t}^2\left(1+\frac{1}{12}W_{zz}\tilde{t}^2\right). \tag{1.2}$$

The initial coordinate and velocity of the test body are $z_0 = z(t_0)$ $v_0 = v(t_0)$, respectively. The $\tilde{t}$ refers to a measured time after correction for light propagation delay correction (Wziontek et al., 2021). The estimation process is highly sensitive to the value of the W_{zz}, which is usually obtained by measuring g-values at different heights over the pillar using a relative gravimeter. On top of that the free fall acceleration estimate is usually reduced to the effective position of the gravimeter which significantly reduces the error related to vertical gravity gradient error (Palinkas et al., 2012). The observations usually take several hours and require more than 1000 free falls depending on the required accuracy. The consecutive free falls of test mass are grouped into sets, represented by a mean value and an error. During the data processing we can selectively include and exclude individual sets in a final value which is determined as a weighted average of sets.

Superconducting gravimeter

A special type of relative gravimeter, a superconducting gravimeter (SG) for use in stationary gravity observations was developed in 1980s. The SG is a relative gravimeter in which the mechanical spring is replaced with a very stable electro-magnetic field and a spherical superconducting test mass (Goodkind, 1999). The magnetic field is produced by two superconducting coils and since there is almost zero resistivity in superconductors, both the persistent currents flowing in the magnet coils and the induced currents in the sphere are ultra-stable and noise free https://www.gwrinstruments.com). Changes in the electric current required to keep the floating sphere in the same position are then used to derive changes in gravity. Maintaining the superconducting state requires an efficient cooling unit capable of keeping the temperature below the transition temperature of the niobium used in the sensor (4 °K). There are currently two SG models manufactured by GWR instruments, the observatory superconducting gravimeter - OSG and a model iGrav which can be deployed in stationary measurements out of the laboratory.

All relative gravimeters are affected by an instrumental drift which due to various factors such as temperature changes, mechanical stress, or aging of components causes artificial changes in measured output over time. Depending on the instrument type, the drift can range from tens to thousands of $nm.s^{-2}.yr^{-1}$. SGs are generally considered as the most stable instruments regarding the drift with long-term linear drift rates for the nine SGs operating in Europe ranging from 16 to 49 $nm.s^{-2}.yr^{-1}$ (Crossley et al., 2005). The drift estimation and correction procedure differ depending on the type of the instrument and will be discussed later within the subsection 1.3.4.
As mentioned earlier, relative gravimeters cannot measure the absolute value of the gravity vector, but rather observe its change by measuring the counterforce required to compensate the gravity change. Therefore, relative gravimeters are subject to a regular calibration process in which an admittance factor (transfer function) is determined between the output units measured by the instrument's automatic feedback system and the units of gravity. The calibration of portable gravimeters often involves measurements on a gravimetric calibration line, for more information see the papers on gravimetric calibration lines (Flury et al., 2006; Sas et al., 2009).

International Geodynamics and Earth Tide Service

The Global Geodynamics Project (GGP) was initiated in the 1980s by the International Association of Geodesy (IAG) to exploit the potential of high-precision gravity measurements and to address the need for unified data processing methodology. Since 2015 the GGP continues as the International Geodynamics and Earth Tide Service (IGETS). The main objective of IGETS is to archive long-term gravity observations and provide monitoring of temporal variations of the Earth gravity field (http://isdc.gfz-potsdam.de/igets-data-base/). Products of the IGETS database can be divided into three levels. Level 1 refers to 1-minute raw gravity and local atmospheric pressure records sampled at 1 or 2 seconds and the same records decimated to 1-minute record. These data sets are provided by the individual station operators of the IGETS network. Ready for use in the tidal analysis, level 2 products are derived from level 1 by correcting for disturbances. Level 3 products are gravity residuals obtained by using particular geophysical corrections (discussed in subsections 1.3.1 to 1.3.4) either with minute or hourly sampling. Optionally, auxiliary data files and station logs are provided by station operators. Auxiliary data files can contain hydrological and meteorological data for scientific investigations, such as groundwater, rainfall or soil moisture. Level 1 to level 3 data are stored in *.ggp format described in (Voigt et al., 2016).

Gravity measurements in hydrological studies

Depending on the type of sensor and used methodology, modern gravimeters are able achieve the accuracy of 10^{-8} to 10^{-9} $m.s^{-2}$ (in some cases even higher). At this rate we observe gravity changes related to non-homogeneous density distribution but also time-variable components of gravity related to environmental phenomena. Phenomena with the largest contribution to the time variation of *g* are tides, effects of atmospheric mass movement and the polar motion effect. These aforementioned effects are commonly removed from all gravity measurements (Timmen, 2010) as the concept of their modelling is generally well-known. The removal of non-hydrological gravity signals from gravity recordings is essential for hydrological applications of gravity measurements. In fact, hydrological signal in gravity recordings only becomes visible after their removal. By correcting gravity time series, we obtain a so-called residual gravity series (gravity residuals). Depending on the location of the site and instrument type, other gravitational and non-gravitational effects such as the non-tidal ocean loading or impact of different length of the day have to be considered.
Before these corrections are applied, the gravity time series have to be filtered using low-pass filter which removes a great portion of environmental noise. A significant part of the environmental noise can be attributed to anthropogenic activities, therefore stationary gravimeters are usually deployed in remote areas where the human activity is lower. To further reduce the environmental noise, stationary gravimeters are often placed on a pillar isolated from the building foundations. While human activities cause an environmental noise with long-term character, earthquakes are responsible for a short-term high frequency noise and perturbations. On top of that, we also have to consider the instrumental noise, which is undistinguishable from the environmental one.
The goal is to remove as much high-frequency signal as possible from the recording. The ETERNA 3.4 package (Wenzel, 1996) provides low-pass zero-phase filters designed for filtering gravity time series. The 1-second to 1-minute filter N01S1M01 has a cut-off time of 300 s, which means that frequencies above ~3 mHz are removed from the record. Hourly gravity data have sufficient temporal resolution for most hydrological applications, except for the analysis of precipitation events. If hourly sampling is desired, additional filtering must be performed, e.g. using ETERNA 3.4 filters N2H1M001 and N14H5M01. Low and high-pass filtration has also been implemented in the TSOFT software along with Butterworth and least-square filtering (Van Camp and Vauterin, 2005).

2 Hydrological signal in gravity measurements

The presence of hydrological signal in gravity recordings has been known since 1970s (Lambert and Beaumont, 1977) when first experiments designed to study gravity changes associated with seasonal groundwater fluctuations were carried out. Despite great efforts during last decades the influence of hydrology doesn't have a unified method of calculation compared to well established methodology for tides, atmosphere and polar motion. This is mainly due

to the fact that we have to deal with multiple hydrological inputs and station specific hydrogeological environment, which makes the generalization process difficult (Kroner et al., 2007). Furthermore, accurate representation of local hydrological conditions requires extensive amount of additional information. For this purpose, individual IGETS sites are usually equipped with additional hydrometeorological sensors.
The whole hydrological signal consists of the direct gravitational (Newtonian) effect of water masses and a smaller indirect effect related to the deformation of the Earth's surface induced by loading of water masses (Romagnoli et al., 2003). The loading effect of water masses is negligible in calculations involving nearby water masses due to its long-wave character (Lampitelli and Francis, 2010). The hydrological signal is a continual function of both the magnitude of hydrological masses and their respective distance to the instrument. However, it is convenient to separate the signal into a global and local component. As stated by authors in (Mikolaj et al., 2015) this approach has its advantages, due to the local component being dominated mainly by a direct effect while at the same time requiring hydrological model with much greater spatial and temporal resolution. Global component on the other hand has to consider both direct and loading effect. Another advantage of this separation is that local hydrological effect (LHE) can have its apex in different time of the year compared to global hydrological effect (GHE). Considering that the influence of the hydrological masses decreases continuously as a function of their size and distance from the gravimeter, the problem arises of clearly defining the areas of each component. The threshold between local and global component is usually set to a spherical distance of 0.1° to 1° from the site (Mikolaj et al., 2015) (Wziontek et al., 2009a). It is important to note that global and local effect may interfere with each other, which complicates the process of their modelling calculating an overall correction accounting for hydrological mass transfers (Wziontek et al., 2009a).

Global hydrological effect

The GHE reflects changes in the distribution of distant hydrological masses associated with the global hydrological cycle, with an approximate annual period. Methods for its calculation are based primarily on global terrestrial hydrological models (GHM), which provide information on changes in hydrological components such as the soil moisture, groundwater level, snow water equivalent (SWE). By summing these hydrological components, we obtain an information about changes in total water storage (TWS) in the form of a grid. According to (Mikolaj et al., 2015) spatial and temporal resolution doesn't have a major influence on the process of calculation, due to great amount of approximation already present in the process. Therefore, the only key component in this process is the accurate representation of the TWS variation in time. A comprehensive tool for the calculation of the global hydrology effect in MATLAB platform (https://www.mathworks.com/products/) has been developed by authors (Mikolaj et al., 2016) to utilize data from various GHMs.

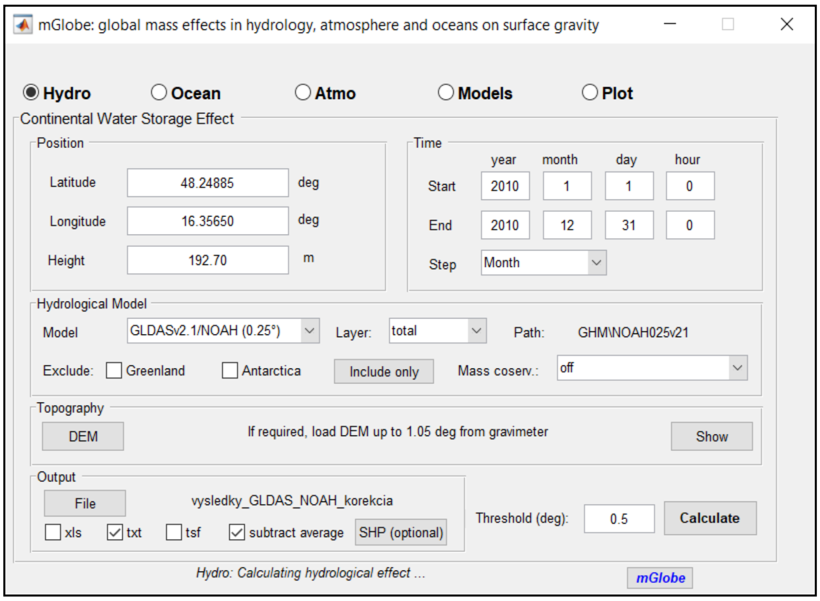

Figure 2.1 The mGlobe graphical user interface.

The tool allows calculatin of global hydrological effect using the following groups of GHMs:

- WaterGAP,
- GLDAS (Global Land Data Assimilation System) models,
- GRACE level 3 products,
- atmosphere reanalysis models e.g. MERRA2 or ERA5,
- and other.

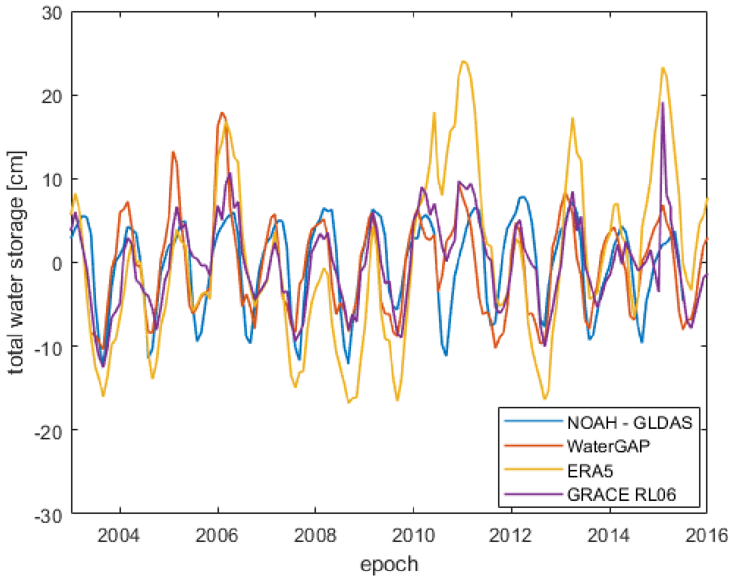

Figure 2.2: Comparison of TWS time series derived from selected GHM for ϕ = 48.5° and λ = 17.5°.

Local hydrological effect

In general, water masses closer to the site produce greater gravity signal than masses located further away. It has been estimated that for some sites up to 90% of the local hydrological signal are due to variations in the amount of hydrological masses within 1000 m of the gravimeter (Creutzfeldt et al., 2008). Given that hydrogeological conditions can often vary over distances of only a few metres, accurate estimation of local hydrological effects requires data with much higher spatial resolution compared to global effect. In addition, water mass transfers at this scale occur at faster rates, which also requires a higher temporal resolution of the data being employed. Due to the integral nature of gravity measurements, we observe variations in the total water mass (TWS) in the vicinity of the gravimeter, which cannot be measured by any other technique. However, the variation of TWS can be divided into individual components that can be monitored and modelled separately, such as soil moisture variations, groundwater variations, snow and ice, amount of water stored in plants and others. Greatest portion the observable hydrological signal comes from changes in the unsaturated and saturated layers, whereas some areas are also influenced by variations of snow cover variation or water stored in surface water bodies. The aim for individual site operators is therefore to identify the source of the observed hydrological signal and to resort to monitoring of individual hydrological components. Physical approaches, on the other hand, rely on an accurate representation of the local distribution of water masses and subsequent Forward Gravity Calculations (FGC). They often combine more than one type of forcing data to produce hydrological models that describe the spatio-temporal distribution of water masses in the local area. The approaches proposed by individual authors differ depending on the type of driving data available and the local hydrogeological conditions at the site, but their common goal is to describe TWS changes in the vicinity of the instrument. Numerical modelling is often used in local hydrological modelling because of the ability to combine different types of input data.

Water balance equation

Water mass balance is an essential aspect of numerical modelling in hydrology and ensures that the hydrological model accurately represents water exchange in the atmosphere-land system. In particular, it links atmospheric processes with subsurface water movements. The water balance equation (2.19) at the catchment scale (Mohajerani et al., 2021) quantifies changes in soil water content by summing rates of inflow and outflow into the unsaturated zone (Byeon, 2014). For any given time interval it includes atmospheric precipitation P_A, evapotranspiration ET and water runoff RO.

$$\Delta TWS = P_A - ET - RO \tag{2.4}$$

In addition, water abstraction and irrigation must be considered in areas affected by human activities. All components of the equation can be expressed either in terms of volume, e.g. [m^3], or in terms of depth per unit of time, e.g. [mm.h^{-1}]. The inflow in equation (2.4) is mainly represented by precipitation, which is any form of water that condenses in the atmosphere and falls to the ground. It is usually measured using a combination of rain and snow gauges. Total runoff consists of a surface runoff, which occurs when precipitation cannot be absorbed by the soil, and a subsurface runoff, which occurs when water percolates into deeper layers of the soil where it reaches the groundwater table and flows horizontally. The Penman-Monteith equation (Monteith, 1965) is widely recognised as the best way of obtaining potential ET rates from meteorological data.

Water mass body approximation

Forward gravity calculations are required for the analysis of the gravity variation originating in the hydrological system. In this case, the forward problem refers to a situation where the gravity field and its variations are calculated from the output of a hydrological model in form of a discrete VWC variations $\theta(z,t)$. Additionally, local topography has to be considered in order to properly describe the spatial distribution of water masses and their relative distance to the instrument. The general geophysical forward problem can be formulated in 3D by integrating equation (1.1) over the area of hydrological system extending from x_{M1}, to x_{M2} and from y_{M1} to y_{M2} in horizontal direction and from z_{M1}, to z_{M2} in vertical direction (Van Camp et al., 2006) as

$$g_w(t) = \int_{x_{M1}}^{x_{M2}} \int_{y_{M1}}^{y_{M2}} \int_{z_{M1}}^{z_{M2}} \frac{G\rho_w\theta(z,t)}{d^2} \cdot \frac{z_0 - z}{d} dxdydz\,, \tag{2.5}$$

where G is the gravitational constant ($6.674 \cdot 10^{-11}$ m^3.kg^{-1}.s^{-2}), ρ_w is the water density (1000 kg.m^{-3}), (x_0, y_0, z_0) is the position of the gravimeter and d is the distance between the instrument and the centre of point mass defined by coordinates (x, y, z):

$$d = \sqrt{(x - x_0)^2 + (y - y_0)^2 + (z - z_0)^2}. \tag{2.6}$$

By horizontally extending the area in eq. (2.5) to ±∞, we obtain a formula (2.7), an infinite layer approximation of water masses analogous to Bouguer's plate (Vanicek et al., 2001), which is suitable for areas with flat topography.

$$g_w(t) = 2\pi\rho_w G H_w(t) \tag{2.7}$$

For LHE calculation it is necessary to take into account the real position of the mass elements relative to the instrument by incorporating their elevation. Assuming, that a Digital Elevation Model (DEM) with sufficient resolution and accuracy is available, the output of a hydrological model can be spatially integrated over the area to form a 3D grid of cells. The state of the art nested grid approach for forward gravity calculation, see (Leiriao et al., 2009) utilizes three different types of mass approximation based on the distance (d) to volume (dr) ratio of each individual cell *f*.

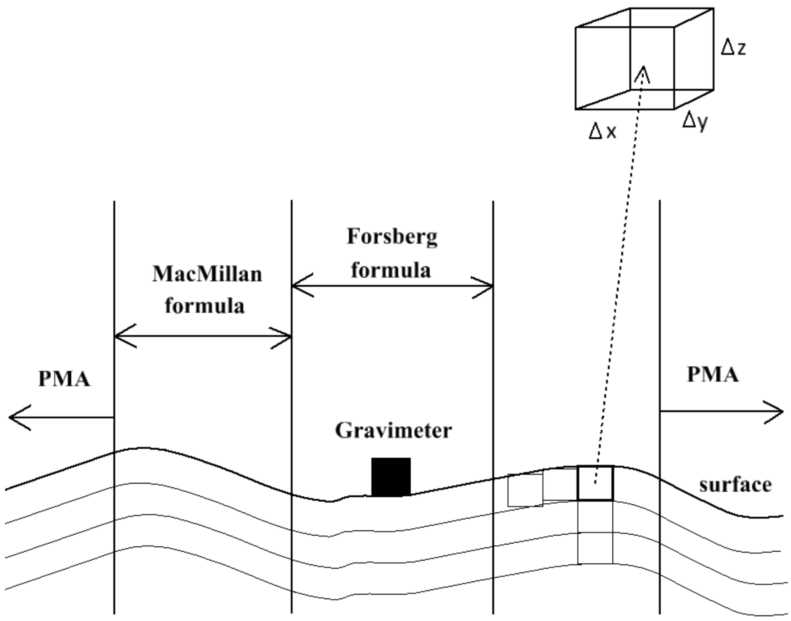

Figure 2.3 Nested grid approach forward gravity calculation classification procedure (Leiriao et al., 2009).

First, each cell is assigned an individual value of f and classified into one of the three groups according to Figure 2.3. For cells located in the vicinity of the instrument ($f^2 < 4$) the algorithm uses the exact prism approximation of the mass element – Forsberg's formula (Forsberg, 1985; Nagy et al., 2000).

$$g_F = G\rho_w\, S_y \left|\left|\left| x\log(y + d) + y\log(x + d) - z\arctan\frac{xy}{zd} \right|_{x_2}^{x_1} \right|_{y2}^{y1} \right|_{z_2}^{z_1}. \tag{2.8}$$

Equation (2.9), often referred to as the MacMillan formula (MacMillan ,1958), is more suitable for intermediate distances for $4 < f^2 < 81$. The use of this formula increases the computational speed in exchange for a lower spatial discretisation. The MacMillan formula approximates the mass element with a spherical harmonics expansion of the prism field:

$$g_M = -G\rho_w S_y \Delta x \Delta y \Delta z \left(-\frac{z}{d^3} - \frac{5}{24}\frac{(\alpha x^2 + \beta y^2 + \omega z^2)z}{d^7} + \frac{1}{12}\frac{\omega z^2}{d^5} \right) \quad (2.9)$$

The individual coefficients α, β, ω used in eq. (2.9) are following:

$$\alpha = 2\Delta x^2 - \Delta y^2 - \Delta z^2 \qquad \beta = \Delta x^2 - 2\Delta y^2 + \Delta z^2 \quad \omega = \Delta x^2 - \Delta y^2 - 2\Delta z^2$$

$$\Delta x = x_2 - x_1 \quad \Delta y = y_2 - y_1 \quad \Delta z = z_2 - z_1.$$

In this formula, *Δx*, *Δy* and *Δz* are the side lengths of the prism, *x*, *y* and *z* are the coordinates of its centre in the system with the origin at the instrument. The prism extends from x_1 to x_2 in the x axis, from y_1 to y_2 in the y axis and from z_1 to z_2 in the z axis. With increasing distance from the instrument, for $f^2 \geq 81$ we can neglect the real size of the element and the associated integration over its volume. Therefore, a three-dimensional Point-Mass Approximation (PMA) can be applied to the grid cells in the rest of the area:

$$g_{PMA} = \frac{G\rho_w S_y \Delta x \Delta y \Delta z}{d^2} \frac{(z - z_0)}{d} \quad (2.10)$$

The specific yield of the mass element S_y is defined as the volume of water that can be contained per unit of volume. Setting the S_y to a value of 1 results in a gravity response of the prism filled with water. For a given location the water admittance factor, (the gravity response of a layer of water of nominal thickness) in nm.s^{-2} per metre is then obtained as the sum of all cell contributions in the horizontal direction and averaged along the vertical (Chaffaut et al., 2020).

Umbrella effect

The gravimeter is usually placed on a concrete pillar in a building to protect it from the outside weather. The building and its foundations act as a shield (umbrella), preventing water from percolating into the underlying soil layers. This alters the natural flow of water and reduces variations in the water content of the soil beneath the building, see e.g. (Reich et al., 2019) or (Creutzfeldt et al., 2010). There are several ways to assess the umbrella effect. The first is to simply exclude the area below the building from the estimation of the admittance factor (see previous chapter). However, this is only viable for a situation where the unsaturated zone is shallow, since all hydrological processes occurring below the building are neglected. The authors in (Kazama et al., 2012) and (Reich et al., 2019) use a separate hydrological model to describe the hydrological processes in the unsaturated zone below the building (see Figure 2.4). It is generally assumed, that no water flow is occurring in the building foundations. However, the soil beneath the building foundations is under the influence of neighboring layers with uninterrupted water flow and groundwater level variations.

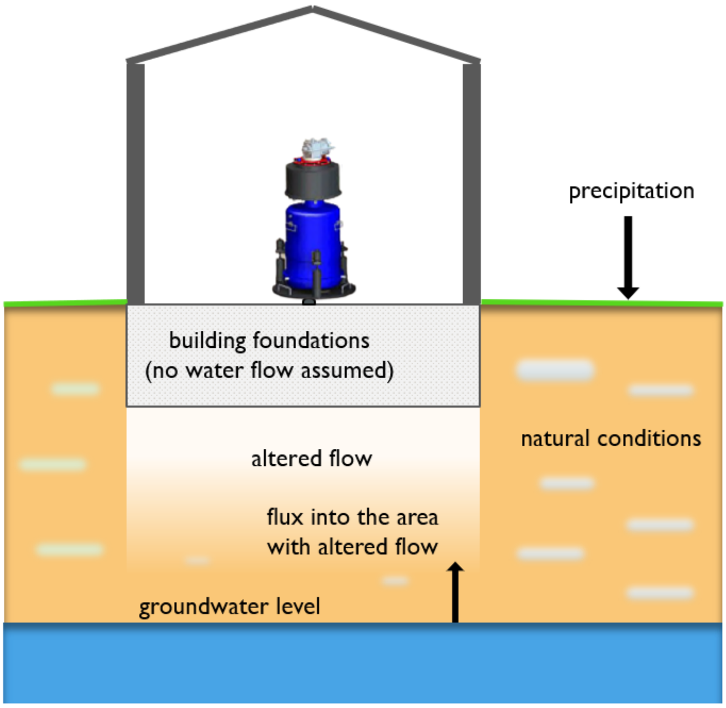

Figure 2.4 The umbrella effect assessment by (Kazama et al., 2012).

3 Practical experiment

Taking into account all the information provided in the previous sections, we have developed a procedure for calculating the hydrological correction that can be followed for an arbitrary site. For the reasons given in section 2, it is divided into a global and a local component. The GHE has been calculated using data from several currently operating GHMs and a comparison of the results is given. For the hydrological model of the unsaturated zone, we use a developed tool that enables forcing of various meteorological data in one model. The main intention was to develop a user-friendly, universally applicable tool for gravimeter operators which with minimum requirements. Since some of sites included in the evaluation process lack the in situ data required for the proposed methodology, we had to explore the option of using alternative source of hydrometeorological data. We explored the use of the global coverage model in LHE calculations and evaluated its performance by comparing it to solutions based on in situ data.
In order to carry out tests representative enough to draw general conclusions, the experiment was carried out on data from both absolute and stationary relative gravimeters. Emphasis was put on the analysis of data from sites stationary gravimeters and especially SGs due to their overall accuracy and long-term stability, which is essential for the analysis of long-term hydrological processes. Data from the following SGs have been analyzed: iGrav33 situated in Müritz National Park (Germany), OSG30 located at Wettzell observatory (Germany) and SG38 located at Río de la Plata (Argentina) In addition, data from a spring gravimeter gPhoneX #108 were used to evaluate the calculated hydrological effect at shorter time spans. Since the developed methodology was first tested at this site, we also provide a detailed description of the site and its surroundings. Finally, gravity measurements carried out with an AG FG5X #247 at points of the Slovak national gravimetric network Ganovce (GANO), Spišské Bystré (SPBY) and Military Unit Kvetnica (VUKV) were used to evaluate the proposed methodology. To assess the effectiveness of the developed correction methodology we compare the variation of gravity residuals decrease in terms of standard deviation before and after applying hydrological correction.

Global hydrological correction

To account for the contribution of distant hydrological masses to value of time-varying gravity we subtract the GHE from the gravity residuals. As stated earlier in section 2.1, the GHE calculation relies on TWS data from GHMs. To assess the performance of various models, we calculate the GHE based on data from three currently operating GHMs: NOAH025 v2.1 (Rodell et al.,2004), ERA5 (Gelaro, 2017) and GRACE-based EWT grids. As the global effect is a long-term phenomenon that can only be observed by a SG due to its inherent stability, the comparison of these models is carried out at sites equipped with SG. Data from the aforementioned models were used in the mGlobe tool (Mikolaj et al., 2016). The tool is written in the MATLAB coding platform (https://www.mathworks.com/) and requires mapping and statistic toolbox. For each of the sites, the threshold between LHE and GHE was set to a spherical distance of 0.1°. The near zone topography was derived from a 90m resolution SRTM model (Jarvis et al., 2008). The monthly NOAH025 v2.1 provides VWC variations in 4 soil layers up to the depth of 2.5 m and snow water equivalent (SWE) with spatial resolution of 0.25°. The ERA5 monthly land model provides SWE and VWC variations in 4 soil layers up to the depth of 2.89 m with spatial resolution of 0.1°.
We have also explored the option of using hydrological models derived from GRACE-FO to force the GHE calculations in mGlobe. Based on earlier tests described in (Novak et al., 2021) we selected the CSR DDK2 monthly sets of SHC with maximum degree of 60 as a base dataset for further calculations. These are available at the ICGEM website (http://icgem.gfz-potsdam.de/home). The poorly estimated C_{20} and C_{30} coefficients were replaced for estimates from satellite laser tracking (Cheng et al., 2013). The SHC were then corrected for the GIA effect (Peltier et al., 2015). Monthly EWT grids with the spatial resolution of 1° were calculated using the modified GrafLab tool (GRAvity Field LABoratory) (Bucha and Janak, 2013).

Local hydrological correction

We have developed a tool that allows the calculation of the local effect resulting from water content changes in the unsaturated zone (SME). The local HydRological effect based On Numerical modelling (HRON) is written in MATLAB R2022a coding platform (https://www.mathworks.com/) that can be accessed using the graphical user interface shown in figure 3.1 or command line interface. The tool uses 1D numerical modelling (see section 2.2.1) driven by hourly effective precipitation in [mm.h^{-1}] to estimate spatiotemporal variations of VWC similar to prior work of (Kazama et al., 2012). It supports import of various formats as provided in example files that can be accessed at (https://github.com/adnovak/HRON). For sites equipped with weather stations, the model input can be calculated according to equation (2.19). To enable SME calculations at sites lacking proper meteorological instrumentation, use of MERRA2 M2T1NXLND with a resolution of 0.5° x 0.625° (https://disc.gsfc.nasa.gov/datasets/M2T1NXLND_5.12.4) is implemented in the tool. Despite the coarser spatial resolution of MERRA2 data and it's much greater approximation, the authors in (Chaffaut et al., 2020) have demonstrated its effectiveness when used in local hydrological modelling. An option to fill in the gaps in the local data is included in the tool. However, the user should

first check whether MERRA2 matches the scale of the local data due to its greater approximation. We compare model output and gravity response driven by both in-situ data and MERRA2 at three sites to assess the effectiveness of using regional scale data to force the local hydrological model.
Due to the use of one-dimensional numerical modelling, the tool is most suitable for areas with flat or near-flat topography, where horizontally homogenous model resembles the real situation. Since the outcome of numerical modelling is highly dependent on the accurate knowledge of soil hydraulic properties, we will provide methods for their determination through analysis of soil samples at the Hurbanovo site. For other sites, the parameters required for the numerical modelling were obtained through calibration of theoretical values given by (Pallin and Kehrer, 2013) by adopting the Monte Carlo method and fitting the modelled VWC variations to measured soil moisture, where available.
The estimated VWC distribution at hourly intervals is then used in forward gravity calculations to obtain the gravitational response of local water masses in the unsaturated zone as seen by the gravimeter. The nested grid approach requires a site-specific admittance factor calculated using equations (2.8) to (2.10) over the DEM grid to be provided by the user. The latter is generally preferred as it also allows us to account for the umbrella effect by selectively excluding grid cells located under buildings.

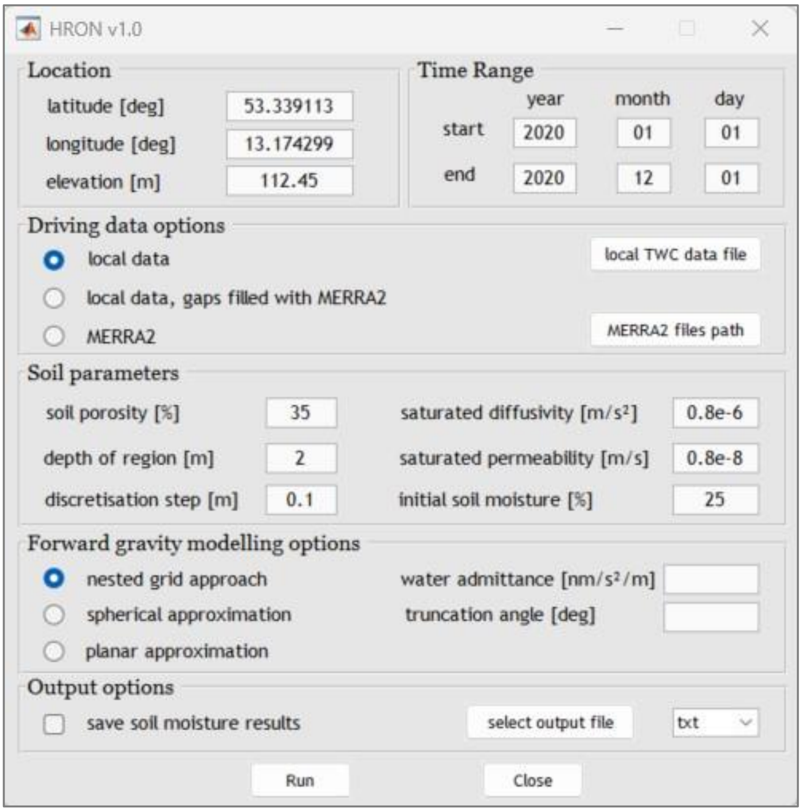

Figure 3.1 Graphical user interface of the developed tool.

Table 0.1 Parameters used for the SME calculations at individual sites.

site	*local data availability*	*depth [m]*	D_s $[m^2.s^{-1}]$	K_s $[m.s^{-1}]$	*P* *[%]*	*water admittance* $[nm.s^{-2}.m^{-1}]$
Hurbanovo	×	2	1×10^{-6}	1.5×10^{-7}	39	419.3
Muritz	✓	13	8.5×10^{-7}	3.8×10^{-9}	20	419.3
Wettzell	✓	3.5	6×10^{-7}	2×10^{-9}	25	109.0
La Plata	✓	12	1.8×10^{-6}	2.8×10^{-8}	40	170.0
Ganovce	×	2	8×10^{-7}	8×10^{-9}	35	327.0
VUKV	×	2	8×10^{-7}	8×10^{-9}	35	292.0
SPBY	×	2	8×10^{-7}	8×10^{-9}	35	242.0

Hurbanovo

To evaluate the modelled hydrological effect, we use data from the Portable Earth Tide (PET) gravimeter gPhoneX #108, stationed at the Hurbanovo Gravimetric Observatory, (Janak et al., 2021). It is located at 47.872°N and 18.193°E with an approximate elevation of 112 m above mean sea level in the Baltic Sea. The terrain in this region, dominated by the Danube lowlands, is generally flat. The gPhoneX uses an automatic aliod beam nulling feedback system, which allows the measurement of gravitational changes equivalent to a level of 1 nm.s^{-2} (Fores et al., 2019). This is equivalent to a gravity response of approximately 2 – 3 mm thick layer of water. However, due to non-linear instrumental drift of up to several thousand nm.s^{-2} per year, high frequency noise and thermal sensitivity, the gPhoneX data are only suitable for the analysis of short-term local hydrological variations. For the LHE evaluation, we use gravity data from a period April to September 2021 with stable gravity observations and sufficient hydrological data.

To account for the thermal sensitivity of the instrument, we use the insulation as shown in Figure 3.2. To further improve the SNR and reduce the thermal sensitivity of the instrument, we have developed a ambient temperature correction procedure that is discussed in (Novak and Janak, 2022). It is important to note that this approach only removes the signal resulting from the movement of the sensors due to thermal expansion, not the drift changes that may also be associated with it. We were unable to estimate the instrumental drift of the gPhoneX #108 by employing simultaneous measurements with the AG according to (Francis et al., 1998) due to high frequency noise of unknown origin (~27 Hz) and insufficient amount of measurements performed. Therefore, we use the least squares adjustment to estimate the linear approximation of the instrumental drift of during the analysed period and subtract it from the gravity residuals.

Figure 3.2 Thermal insulation of the gPhoneX #108.

In order to monitor local meteorological and hydrological parameters, the Hurbanovo gravimetric observatory is equipped with several sensors. The MWS9-5 weather station is located in the immediate vicinity of the observatory and provides meteorological data at 1 minute intervals. Unfortunately, during this period, the weather station recorded a 12-hour precipitation average, which does not provide sufficient temporal resolution for the methodology we have developed As a result, we are limited to using other sources of rainfall data for this site. Groundwater level variation is monitored at 5-minute intervals by a sensor located in a groundwater well beneath the weather station. To match the temporal resolution of the analysed gravity dataset, the groundwater data are decimated to hourly time series. In addition, a total of 8 TMS-4 sensors, which enable the measurement of VWC (Wild et al., 2019), have been deployed in 4 pairs in the vicinity of the building since July 2020, as shown in Figure 3.2. More than 30 undisturbed soil core samples were extracted during the installation of TMS-4 sensors at their exact location. Since the sample remains intact and representative of the in-situ soil conditions, including the soil texture, structure, and moisture content it can be used to derive the soil hydraulic properties required for numerical modelling. Kopecky cylinders (Usowic and Lipiec, 2019) were used for the transfer between the field and the laboratory. Due to long transfers between the field and the laboratory, only 3 of the samples were in condition that allowed them to be analysed. The soil samples were first analysed to determine the saturated hydraulic conductivity K_s.

The estimated values ranged from 0.9 to 2×10^{-7} m.s^{-1}. The average estimated porosity P was 39%, which is in accordance with the expected values for sandy clay loam soils (see soil texture triangle in Appendix B). For the saturated diffusivity D_s we use a value of 1×10^{-6} m.s^{-2} based on (Liu et al., 2009). For the initial condition, we use the average VWC at the start of the calculation from all TMS-4 sensors. Alternatively, the NOAH025 v2.1 hourly model provides surface SM values to start the SME calculations. The aforementioned parameters were used for the numerical modelling in the developed tool between April and October 2021. We initiate the model calculations in October 2020 to include a 6 month warm up period. The output of the hydrological model in terms of VWC variations was compared with the variations measured by the TMS-4 sensors. For comparison, measurements from near-surface sensors and sensors deployed at 1 to 1.1 m depth were averaged. Correlation coefficients of 0.87 and 0.97 between measured and modelled VWC variations were estimated for upper and lower sensors and modelled VWC time series, respectively.

To transfer the numerically modelled water content in unsaturated zone to units of gravity, we have calculated a water admittance factor according to (Leiriao et al., 2009). For this we have utilized a DEM of the local area, the DTM5.0 (UGKK SR, online) based on airborne LIDAR measurements with spatial resolution of 0.25 m and overall accuracy better than 10 cm. To account for the umbrella effect, we have excluded all grid cells located below structures (see Figure 3.3) that disrupt the natural flow of water such as buildings or roads. Since we don't have any information about the individual buildings foundations' depth we were restricted to this approach. We provide a unmasked effect which doesn't accounts for umbrella effect and a masked effect as a function of integration radius in Figure 3.4. The unmasked water admittance reaches the ~419 nm.s^{-2}.m^{-1} of water at integration radius of few hundred metres, and ~ 375 nm.s^{-2}.m^{-1} after accounting for umbrella effect. It is evident that more than 90% of the local hydrological signal originates within the area with distance less than 100 m.

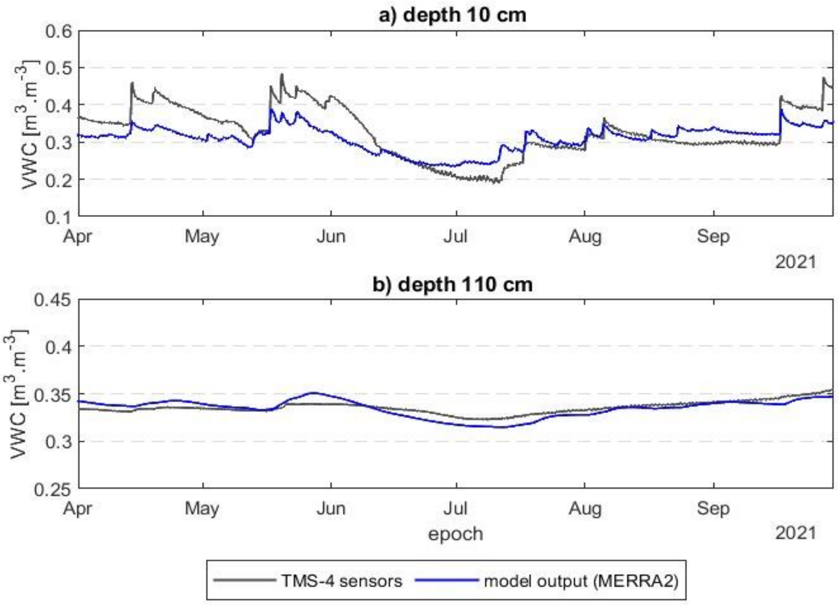

Figure 0.3 Hydrological model output compared with measured VWC variation at Hurbanovo site at depth a) 10cm and b) 110 cm. Modelled VWC variations are shown in blue and measured in black.

.

Using the estimated water admittance factor, that includes the umbrella effect (375 nm.s^{-2}.m^{-1}), the output of the hydrological modelling is transferred to units of gravity effectively resulting in the SME comparable to gravity residuals g_r. Since, the instrument is only suitable for analysis of short-period changes, we have corrected the gravity residuals for GHE calculated using data from the NOAH025 v2.1 and GWE by subtracting them from the g_r. The GHM choice has little effect for a period of only few months, resulting in discrepancies of less than 0.1 nm.s^{-2}. For the GWE calculation, we utilized the groundwater level variation data from the nearby well with S_y approximated by the site specific porosity also used for the numerical modelling (P = 0.39). Results are presented in Figure 3.5 in three subsecutive steps a) to c), following the order of data correction procedure. Overall, the subtraction of all three effects resulted in a 50% reduction in the standard deviation and a reduction in the range from 151 to 86 nm.s^{-2}. The SME correction accounts only for 14 % of the total reduction, mainly due to a greater approximation of MERRA2 data used to force the simulations. Nevertheless, this demonstrates that the global scale model is a viable substitute for in-situ data at sites lacking proper hydrometeorological instrumentation. Figure 3.5 also shows, that despite the higher noise present in the gPhoneX gravity measurements, they are still capable of detecting hydrological mass redistributions that occur over short periods of time. After subtracting all three effects, there is still a lot of unexplained signal in the gravity residuals present, however we couldn't relate it to any other hydrological source.

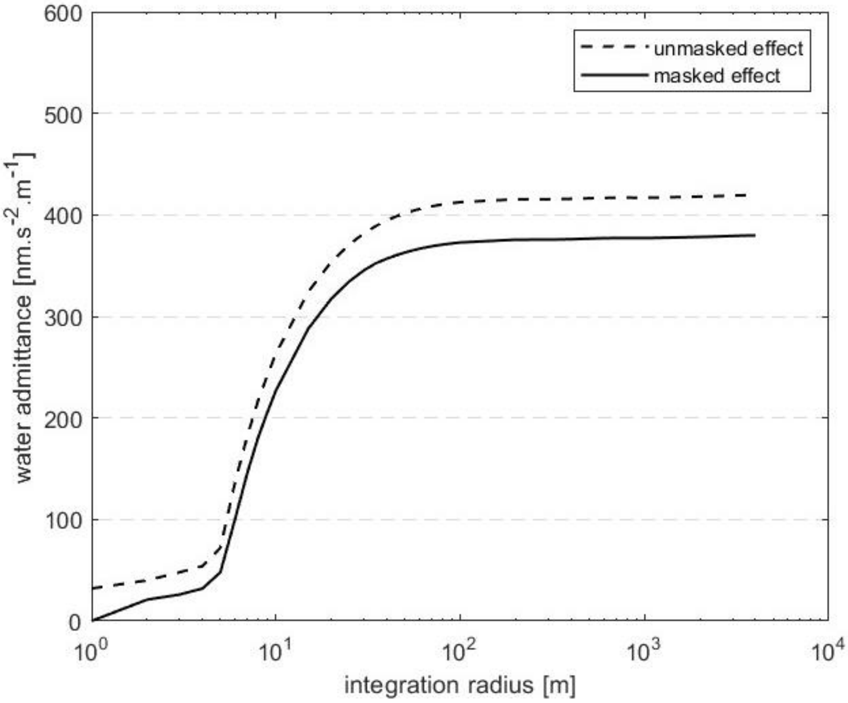

Figure 3.4 Hurbanovo site specific water admittance calculated using the nested grid approach. Dotted line represents unmasked effect, which neglects the umbrella effect. The solid line represents the masked effect, which accounts for the umbrella effect of the observatory building and nearby structures.

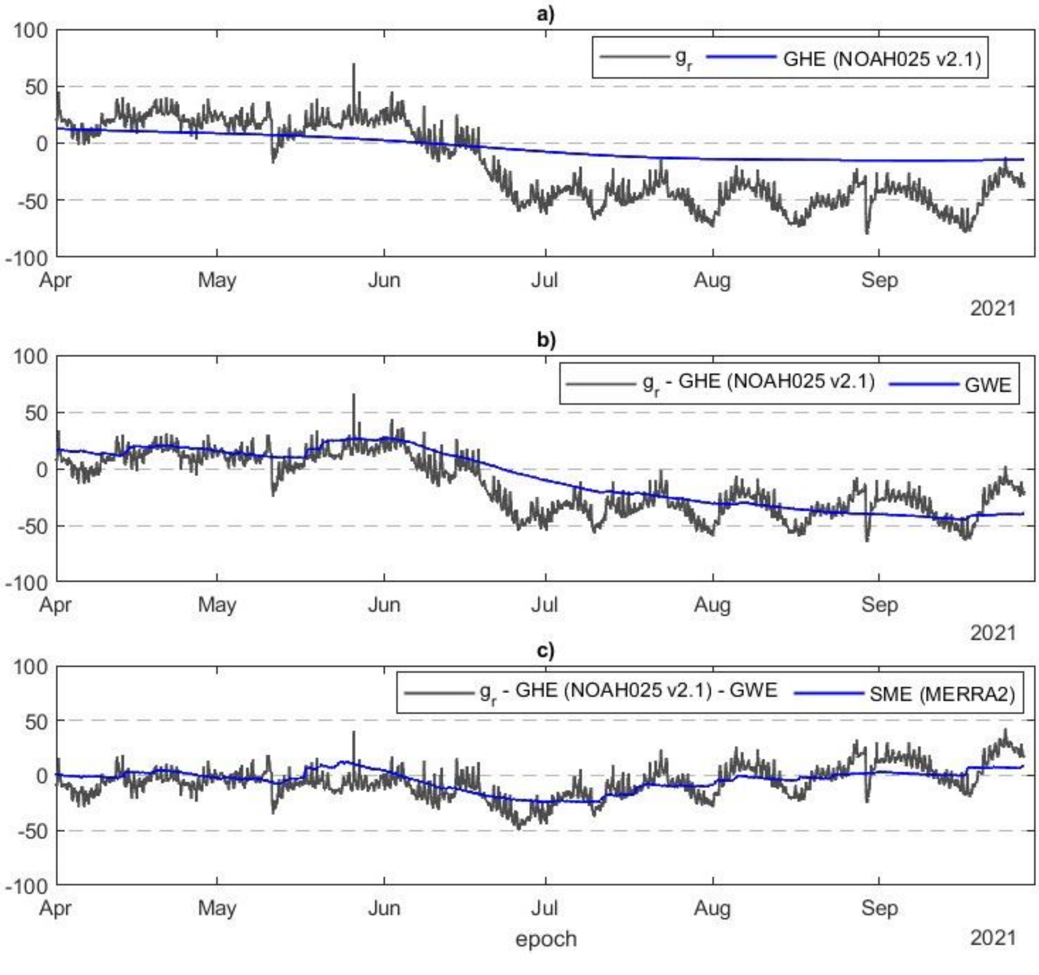

Figure 0.5 a) The gPhoneX #108 hourly gravity residuals compared with GHE calculated using NOAH025 v2.1, b) residuals after subtracting the GHE compared with the GWE, c) residuals after subtracting GHE and GWE compared with the SME driven by MERRA2.

Muritz

The iGrav#33 used for the evaluation is located at the TERENO site in the Muritz National Park in Germany at approximately 53.340 °N and 13.176 °E at an altitude of 112 m (TERENO, online). It was established in and is currently operated by the GFZ. Due to its remote rural location, the station is characterized by low environmental noise. To support the hydrological studies, the site is equipped with a weather station, SM sensors and groundwater well with a sensor to measure groundwater variations. The terrain of the national park area is relatively flat, and previous estimates have shown that the infinite layer approximation is suitable for FGC with respect to the effect of hydrological masses. The instrument is installed directly in a field on a concrete pillar of approximately 1x1 m in size, which produces a negligible umbrella effect.

Due to the proximity of the site to the ocean, an additional NTOL correction is applied to the gravity residuals in addition to the standard corrections. The LOD correction is also included in the g_r preparation due to the higher accuracy of the SG. The instrumental drift was estimated from simultaneous SG and AG measurements carried out at the site prior to data analysis. The GHE is calculated using the three monthly GHMs, NOAH025 v2.1, ERA5 and GRACE-based EWT grids. The use of GRACE-based EWT grids produces reasonable results despite relying solely on GGMs, however, they tend to slightly underestimate the GHE compared to standard models. As the GHE based on ERA5 data removes the greatest amount of signal (~ 30 %), we subtract it from the residuals before further comparison with GWE and SME. In comparison, the GHE based on NOAH025 v2.1 removes only 28% of the signal and the GHE based on GRACE-FO data removes 26%. The GWE was calculated using the groundwater level variation data from a nearby well with the S_y approximated by the site-specific *P* provided in table 3.1. The SME calculations were forced by a local *ΔTWS* neglecting the water runoff. Gaps in the local data were filled by MERRA2 data.

A comparison of the measured VWC variations with the hydrological model output is provided in Appendix C. The modelled SME yields a correlation coefficient of 0.92 and 0.87 with gravity residuals after subtracting GHE and GWE for solutions based on local data and MERRA2 data respectively. A 55% reduction in the variation of the gravity residuals is achieved by subtracting the SME driven by the local data and 49% when the MERRA2-driven SME is removed. Subtracting all three effects reduces the variation of gravity residuals by 62% and reduces the range of data by 56%.

Wettzell

The Geodetic Observatory Wettzell in Germany was established in 1972 as a joint project of the Federal Agency for Cartography and Geodesy (BKG) and the Technical University of Munich. The Geodetic Observatory Wettzell is located in rural area on a mountain ridge of the Bavarian Forest at 12.88° E, 49.10° N at 611 m above the mean sea level. The OSG#30 used for the evaluation has been situated at one of the observatory buildings since 2010 and provides data through the IGETS. The observatory is equipped with an extensive amount of auxiliary meteorological and hydrological instrumentation such as weather station, a lysimeter and SM sensors (Wziontek et al., 2017). Data from this site have already been used in studies related to the analysis of hydrological phenomenon using gravity. See e.g. (Creutzfeldt et al., 2008) or (Reich et al., 2019), where the authors also provide a detailed description of the site, its surroundings and sensor placement. A previous study by (Creutzfeldt et al., 2010) showed that for this site up to 90% of the local hydrological signal originates from the area within 1000 m of the instrument.

The long term stability of OSG gravimeters allows the evaluation of different GHMs in the process of GHE calculation. Similar to Muritz, the best performing GHM is the ERA5, which provides a g_r variation reduction of 30%, 29% in the case of NOAH025 v2.1 and 21% for GRACE-FO. The GWE was calculated using the groundwater level variation data from a nearby well 'BK14' with the S_y provided in (Creutzfeldt et al., 2010). A Comparison of the g_r after subtracting GHE based on ERA5 with modelled GWE is shown in Figure 3.7. A subtraction of GWE from the g_r yielded a 25% decrease of variations. We calculate the SME based on both local ΔTWS and MERRA2 data. For the local data, hourly precipitation is measured by a weather station and ET is measured by a lysimeter located near the observatory. The combined GWE and SME correspond to about 70% of the total hydrological signal observed by OSG#30, confirming previous studies of the hydrological effect at the Wettzell observatory.

By subtracting the locally driven SME, we achieve a 38% reduction in variation of g_r and an 18% reduction using the MERRA2-driven SME. In total, all three corrections removed as much as 70% of the variation and reduced the data range by up to 55%. The slightly worse performance of MERRA2 can be explained by the second half of 2022, where the modelled SME doesn't reflect the significant increase of 20 $nm.s^{-2}$ associated with local hydrological masses. This can be attributed to the spatial resolution of the MERRA2 and its approximation over a larger area.

La Plata

The OSG#38 used for the evaluation has been stationed at Argentinian-German Geodetic Observatory (AGGO) since 2015 as a joint project of the Argentinean National Scientific and Technical Research Council, BKG and GFZ. The site is located in La Plata (Buenos Aires) at 58.14° W, 34.87° S, at the elevation of 25 m. The instrument is placed on a pillar with a 5 m deep foundation in a room thermally stabilised by air conditioning. In 2017, the site has become part of the IGETS, providing nearly uninterrupted gravity time series (Wziontek et al., 2017). In addition, the AGGO is equipped with a weather station, soil moisture sensors, vertical soil moisture profiles to monitor changes in water storage in the vicinity of the gravimeter, and two groundwater monitoring wells. The site specific S_y of 0.11 was estimated in a previous study (Pendiuk et al., 2020) using the hydrogravimetric method.
The SME calculations were driven by local hourly ΔTWS data (see Appendix C) obtained by subtracting calculated ET from hourly precipitation. The terrain surrounding the AGGO is flat, but due to its urban location, a significant umbrella effect affects the local hydrological processes. We resort to this approach due to the lack of detailed knowledge of individual building foundations and the depth of the unsaturated zone of 12 m used for the modelling. The value of 170.0 nm.s^{-2}.m^{-1} suggests a presence of significant umbrella effect, as otherwise we would expect a value close to 419 nm.s^{-2}.m^{-1} in areas with similar topography. The full three step correction reduced a the g_r variations by 65% (49% for SME driven by MERRA2) and reduced the range of the data by 52 % and 43% respectively. However, looking at the large events in Figure 3.7 where the observed gravity increased, we can see that SME underestimated the true signal. This is also confirmed when comparing the modelled and measured VWC for this site. Furthermore, the MERRA2-driven SME failed to capture the decrease in gravity recorded by the SG in the first half of 2021, instead showing an increase.

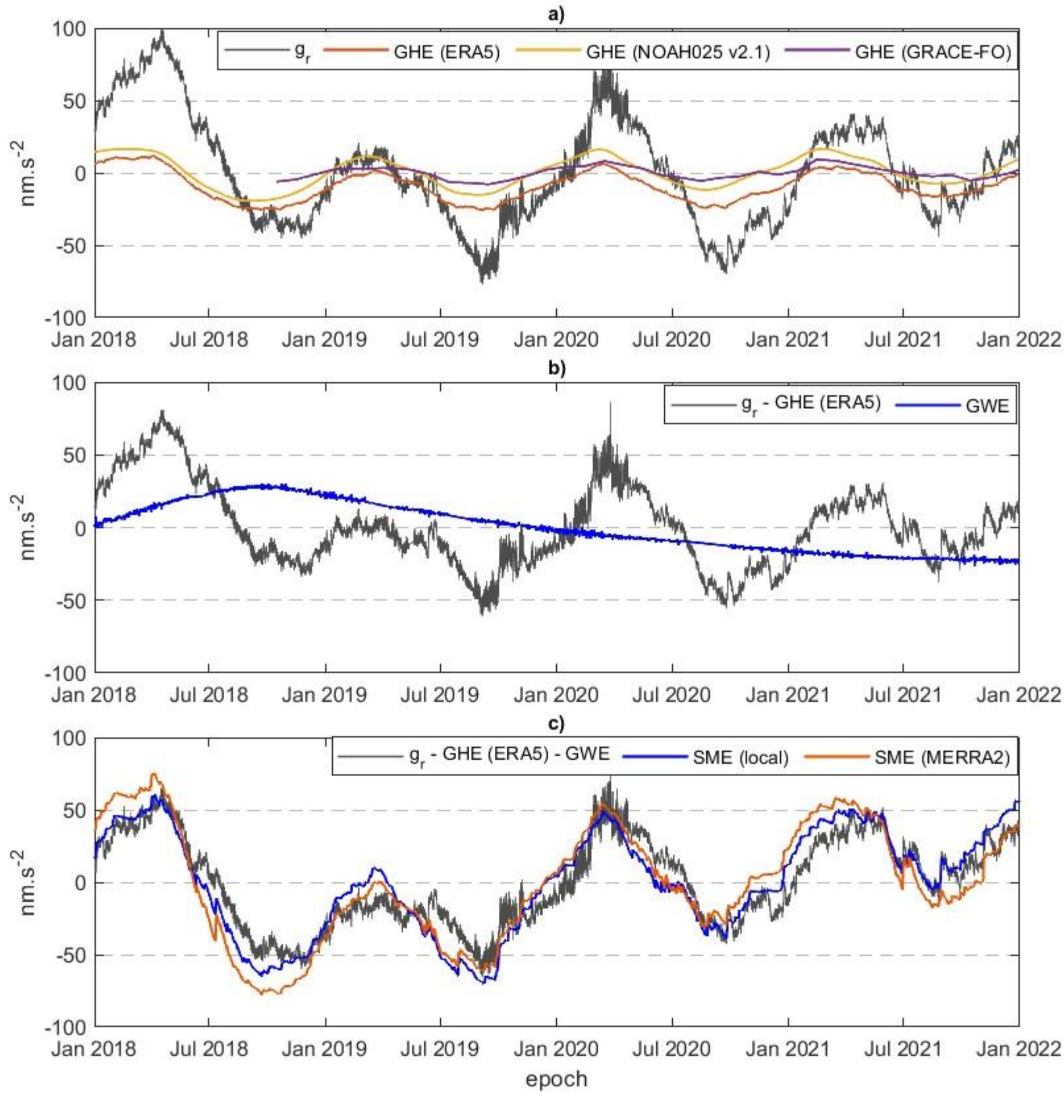

Figure 0.6 The iGrav#33 gravity residuals compared with the GHE calculated using NOAH025 v2.1, ERA5 and GRACE-FO data, b) gravity residuals after subtracting GHE (ERA5) compared with the GWE, c) gravity residuals after subtracting the GHE and the GWE compared with the SME driven by local and MERRA2 data.

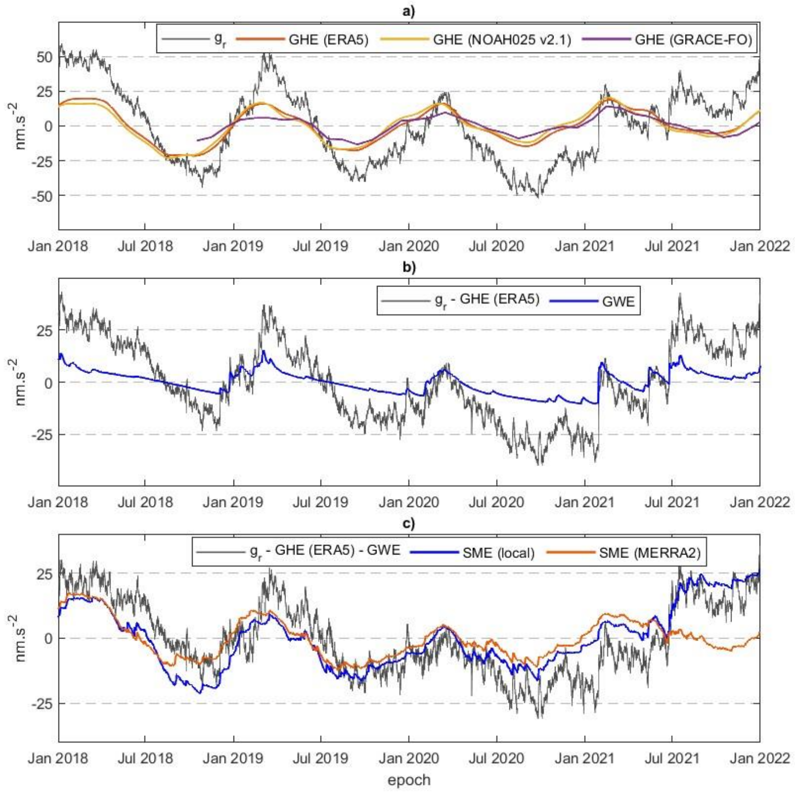

Figure 0.7 The OSG#30 hourly gravity residuals compared with the GHE calculated using NOAH025 v2.1, ERA5 and GRACE-FO data, b) gravity residuals after subtracting the GHE (ERA5) compared with GWE, c) gravity residuals after subtracting the GHE and the GWE compared with the SME driven by local and MERRA2.

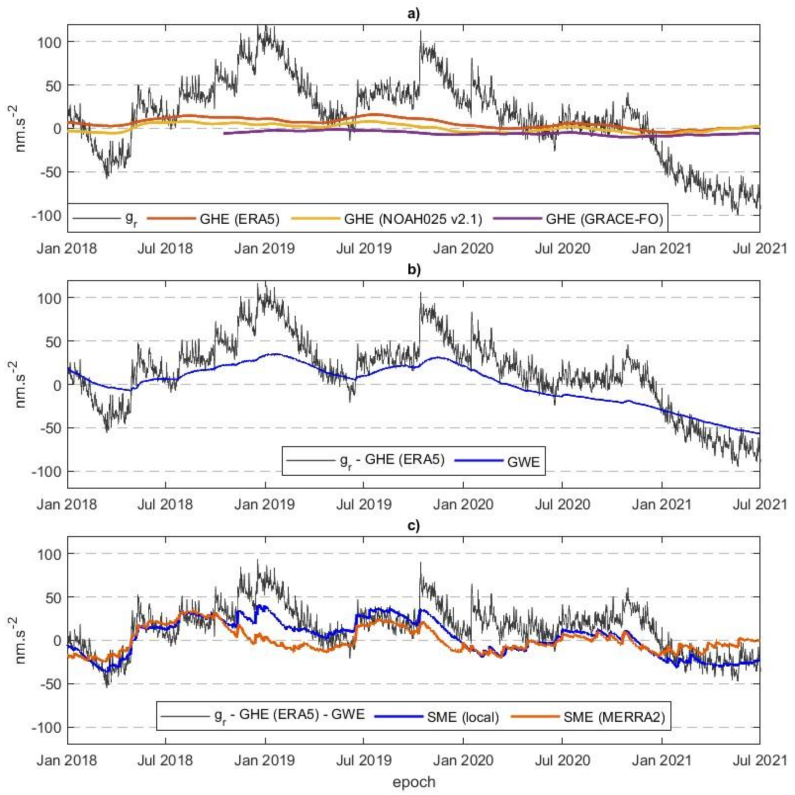

Figure 0.8 The OSG#38 hourly gravity residuals compared with the GHE calculated using NOAH025 v2.1, ERA5 and GRACE-FO data, b) gravity residuals after subtracting the GHE (ERA5) compared with the GWE, c) residuals after subtracting the GHE and the GWE compared with the SME driven by local and MERRA2.

Conclusions

The aim of this thesis was to analyse the influence of hydrological redistribution on terrestrial gravimetric measurements. Due to the magnitude of the gravitational signal it produces, hydrology is considered to be one of the most important phenomena contributing to time variable gravity. As shown on several occasions in this thesis, the hydrological signal significantly exceeds the accuracy of current gravimeters and should therefore be considered prior to any non-hydrological analysis. Most of the observed hydrological signal is produced by the redistribution of water masses in the unsaturated and the saturated zone in the vicinity of the instrument. Methods commonly used to reduce the influence of water mass redistribution on gravity measurements are reviewed and their advantages are discussed.

A correction procedure has been developed that can be applied at any site to remove a significant proportion of the hydrological effect from gravity measurements. For the gravitational effect of distant water masses and their deformation effect we use data from currently operating models NOAH025 v2.1 and ERA5. We have also investigated the possibility of using monthly gravity models based on GRACE-FO data in the GHE calculation process. Comparison with SG measurements shows that GRACE-FO is a viable replacement for traditional GHMs. However, as shown in the work it was outperformed by ERA5 at all the sites. The second component takes into account the gravitational effect of groundwater level variations in the vicinity of the instrument. As we show, the groundwater level variations monitored at the site together with the specific yield can provide sufficient results. The last component covers the influence water mass redistributions that occur in the unsaturated soil layer.

For this purpose, we have developed a tool Local HydRological effect based On the Numerical modelling (HRON), written in MATLAB platform. The tool uses 1D numerical modelling driven by hourly effective precipitation defined by the catchment-scale water balance equation. The potential use of global MERRA2 in the tool as driving data enables applications in locations where hydrological instrumentation is absent or very little information is known. The soil parameters required for numerical modelling can either be obtained by analysing soil samples or estimated by calibrating theoretical values by fitting model soil moisture to in-situ measurements. As we show in our work, the 1D hydrological model provides a reasonable approximation of hydrological processes even in areas without flat topography. The output of the hydrological model is converted to units of gravity using one of three forward gravity calculation options. The first option requires knowledge of the site-specific water admittance factor based on the DEM of the area. The second option is the approximation of water masses by a truncated spherical shell, which constrains the horizontal extent of the infinite water layer provided as the third option.

To assess the effectiveness of the developed tool we compare the modelled hydrological effect with data from various gravimeters. We put emphasis on analysing data from superconducting gravimeters, since their accuracy and long-term stability is essential for the study of long-term hydrological mass redistributions. Additionally, we analyse measurements carried out by the spring gravimeter gPhoneX#108 and the absolute gravimeter FG5X #247. We show, that under specific conditions the gPhoneX gravimeter is able to observe water mass redistributions and the associated gravity signal over short periods of time. For this, we have developed a method to correct the gPhoneX data for the effect of ambient temperature which can overshadow the hydrological processes during analyses.

For all sites included in the evaluation, the magnitude of the local effect exceeded that of the global effect, confirming the importance of investigating the local effect where possible. The SME correction calculated in our tool was able to remove up to 55% of the residual gravity variation when driving data based on in-situ observations were used, and significantly reduced gravity variations related to short and long-term hydrological processes. As shown in our work, the use of MERRA2 data, which have a much higher degree of approximation in numerical modelling, has resulted in good agreement with simulations that are driven by in-situ data. Another global model providing hourly precipitation data that is worth testing further is ERA5. However, at the time of writing, the model contained many artefacts and proved to be insufficient. Future plans include incorporating the estimation of the water admittance factor into the developed tool based on the DEM provided by the user.

References

ALLEN, R. G., WALTER, I. A., ELLIOTT, R. L., HOWELL, T. A., ITENFISU, D., JENSEN, M. E. AND SNYDER, R. L., 2005. The ASCE Standardized Reference Evapotranspiration Equation. American Society of Civil Engineering Reston, Virginia, p. 192.

AN, N., HEMMATI, S. and CUI, Y. J., 2017. Assessment of the methods for determining net radiation at different time-scales of meteorological variables. *Journal of Rock Mechanics and Geotechnical Engineering*. Online. April 2017. Vol. 9, no. 2, p. 239–246. DOI 10.1016/j.jrmge.2016.10.004.

ANDO, B. and CARBONE, D., 2001. A methodology for reducing the effect of meteorological parameters on a continuously recording gravity meter. *IEEE Transactions on Instrumentation and Measurement*. Online. October 2001. Vol. 50, no. 5, p. 1248–1254. DOI 10.1109/19.963193.

BANDIKOVA, T. and FLURY, J., 2014. Improvement of the GRACE star camera data based on the revision of the combination method. *Advances in Space Research*. Online. November 2014. Vol. 54, no. 9, p. 1818–1827. DOI 10.1016/j.asr.2014.07.004.

BYEON, S. J., 2014. Water balance assessment for stable water management in island region. Doctoral dissertation, Université Nice Sophia Antipolis

CG-6 AutogravTM gravity meter. *Micro-g LaCoste* [online]. 17 September 2021. [Accessed May 2023]. Available from: https://microglacoste.com/product/cg-6-autograv-gravity-meter/.

CHAFFAUT, Q., HINDERER, J., MASSON, F., VIVILLE, D., BERNARD, J. D., COTEL, S., PIERRET, M. C., LESPARRE, N. and JEANNOT, B., 2020. Continuous Monitoring with a Superconducting Gravimeter As a Proxy for Water Storage Changes in a Mountain Catchment. In: FREYMUELLER, J. T. and SÁNCHEZ, L. (eds.), *Beyond 100: The Next Century in Geodesy*. Online. Cham: Springer International Publishing. p. 261–267. ISBN 9783031098567.

CHEN, J., CAZENAVE, A., DAHLE, C., LLOVEL, W., PANET, I., PFEFFER, J. and MOREIRA, L., 2022. Applications and Challenges of GRACE and GRACE Follow-On Satellite Gravimetry. *Surveys in Geophysics*. Online. February 2022. Vol. 43, no. 1, p. 305–345. DOI 10.1007/s10712-021-09685-x.

CHENG, M, TAPLEY, B. D. and RIES, J. C., 2013. Deceleration in the Earth's oblateness: J2 VARIATIONS. *Journal of Geophysical Research: Solid Earth*. Online. February 2013. Vol. 118, no. 2, p. 740–747. DOI 10.1002/jgrb.50058.

CHRISTIANSEN, L., BINNING, P., ANDERSEN, O., BAUER-GOTTWEIN, P., 2009. Spatial and Temporal Gravity Data Used for Hydrological Model Calibration: Field Study of a Recharge Event in the Okavango Delta, Botswana. EOS, Trans. American geophysical Union. 11. 4194.

COOK, A. H., 1967. A new absolute determination of the acceleration due to gravity at the National Physical Laboratory, England. Phil. Trans. Roy. Soc., London, A261, p. 211-252.

COPERNICUS CLIMATE CHANGE SERVICE, 2019. *ERA5-Land monthly averaged* data from 2001 to present. Online. 2019. ECMWF. [Accessed 16 May 2023].

CREUTZFELDT, B., GUNTNER, A., KLUGEL, T., WZIONTEK, H. 2008. Simulating the influence of water storage changes on the superconducting gravimeter of the Geodetic Observatory Wettzell, Germany. Geophysics. 73 (6).

CREUTZFELDT, B., GÜNTNER, A., WZIONTEK, H. and MERZ, B., 2010. Reducing local hydrology from high-precision gravity measurements: a lysimeter-based approach: Reducing hydrology from gravity measurements. Geophysical Journal International. Online. October 2010. Vol. 183, no. 1, p. 178–187. DOI 10.1111/j.1365-246X.2010.04742.x.

CROSSLEY, D., HINDERER, J. and BOY, J. P., 2005. Time variation of the European gravity field from superconducting gravimeters. Geophysical Journal International. Online. Vol. 161, no. 2, p. 257–264. DOI 10.1111/j.1365-246X.2005.02586.x.

DAMIATA, B. N. and LEE, T. C., 2006. Simulated gravitational response to hydraulic testing of unconfined aquifers. Journal of Hydrology. Online. March 2006. Vol. 318, no. 1–4, p. 348–359. DOI 10.1016/j.jhydrol.2005.06.024.

DARCY, H., 1856. Les fontaines publiques de la ville de Dijon. Paris: Dalmont.

DEHANT, V., DEFRAIGNE, P. and WAHR, J. M., 1999. Tides for a convective Earth. Journal of Geophysical Research: Solid Earth. Online. 10 January 1999. Vol. 104, no. B1, p. 1035–1058. DOI 10.1029/1998JB900051.

DOLL, P., LEHNER, B., KASPAR, F., 2002. Global Modelling of Groundwater Recharge

DUCARME, B., SUN, H. P. and XU, J. Q., 2007. Determination of the free core nutation period from tidal gravity observations of the GGP superconducting gravimeter network. Journal of Geodesy. Online. 23 February 2007. Vol. 81, no. 3, p. 179–187. DOI 10.1007/s00190-006-0098-9.

Earth Orientation Parameters. *IERS* [online]. [Accessed May 2023]. Available from: https://www.iers.org/IERS/EN/DataProducts/EarthOrientationData/eop.html.

ELSAKA, B., FRANCIS, O. and KUSCHE, J., 2023. Calibration of the Latest Generation Superconducting Gravimeter iGrav-043 Using the Observatory Superconducting Gravimeter OSG-CT040 and the Comparisons of Their Characteristics at the Walferdange Underground Laboratory for Geodynamics, Luxembourg. Pure and Applied Geophysics. Online. February 2023. Vol. 180, no. 2, p. 629–641. DOI 10.1007/s00024-021-02938-1.

Engineering simulation software | ansys products. *ANSYS* [online]. [Accessed May 2023]. Available from: https://www.ansys.com/products.

FALLER, J. E., 1965 Results of an absolute determination of the acceleration of gravity. *Journal of Geophysical Research* 70, p. 4035-4038.
FAMIGLIETTI, J. S., RYU, D., BERG, A. A., RODELL, M. and JACKSON, T. J., 2008. Field observations of soil moisture variability across scales: Soil Moisture Variability Across Scales. *Water Resources Research*. Online. January 2008. Vol. 44, no. 1. DOI 10.1029/2006WR005804.
FARRELL, W. E., 1972. Deformation of the Earth by surface loads. *Reviews of Geophysics*. Online. 1972. Vol. 10, no. 3, p. 761. DOI 10.1029/RG010i003p00761.
FARTHING, M. W. and OGDEN, F. L., 2017. Numerical Solution of Richards' Equation: A Review of Advances and Challenges. *Soil Science Society of America Journal*. Online. November 2017. Vol. 81, no. 6, p. 1257–1269. DOI 10.2136/sssaj2017.02.0058.
FENG, W., 2019. GRAMAT: a comprehensive Matlab toolbox for estimating global mass variations from GRACE satellite data. *Earth Science Informatics*. Online. September 2019. Vol. 12, no. 3, p. 389–404. DOI 10.1007/s12145-018-0368-0.
Field Application Gravity Meters - *GWR Instruments, Inc*. - San Diego, California. Online. [Accessed 22 May 2023]. Available from: https://www.gwrinstruments.com/.
FLURY, J., PETERS, T., SCHMEER, M., TIMMEN, L., WILMES, H., FALK, R., 2006. Precision gravimetry in the new Zugspitze gravity meter calibration system.
FORES, B., KLEIN, G., LE MOIGNE, N. and FRANCIS, O., 2019. Long-Term Stability of Tilt-Controlled gPhoneX Gravimeters. *Journal of Geophysical Research: Solid Earth*. Online. November 2019. Vol. 124, no. 11, p. 12264–12276. DOI 10.1029/2019JB018276.
FORSBERG, R., 1985. Gravity field terrain effect computations by FFT. Bull. Geodesique 59, p. 342–360. DOI 10.1007/BF025210.
FRANCIS, O., NIEBAUER, T. M., SASAGAWA, G., KLOPPING, F. and GSCHWIND, J., 1998. Calibration of a superconducting gravimeter by comparison with an absolute gravimeter FG5 in Boulder. *Geophysical Research Letters*. Online. 1 Vol. 25, no. 7, p. 1075–1078. DOI 10.1029/98GL00712.
FRANZ, T. E., WAHBI, A., VREUGDENHIL, M., WELTIN, G., HENG, L., OISMUELLER, M., STRAUSS, P., DERCON, G. and DESILETS, D., 2016. Using Cosmic-Ray Neutron Probes to Monitor Landscape Scale Soil Water Content in Mixed Land Use Agricultural Systems. *Applied and Environmental Soil Science*. Online. 2016. Vol. 2016, p. 1–11. DOI 10.1155/2016/4323742.
GARDNER, W. R. and MAYHUGH, M. S., 1958. Solutions and Tests of the Diffusion Equation for the Movement of Water in Soil. *Soil Science Society of America Journal*. Online. May 1958. Vol. 22, no. 3, p. 197–201. DOI 10.2136/sssaj1958.03615995002200030003x.
GEHMAN, C. L., HARRY, D. L., SANFORD, W. E., STEDNICK, J. D. and BECKMAN, N. A., 2009. Estimating specific yield and storage change in an unconfined aquifer using temporal gravity surveys: ESTIMATING AQUIFER PROPERTIES. *Water Resources Research*. Online. April 2009. Vol. 45, no. 4. DOI 10.1029/2007WR006096.
GELARO, R., et al., 2017. The Modern-Era Retrospective Analysis for Research and Applications, Version 2 (MERRA-2). *Journal of Climate*. Online. July 2017. Vol. 30, no. 14, p. 5419–5454. DOI 10.1175/JCLI-D-16-0758.1.
GES DISC NASA [online]. [Accessed May 2023]. Available from: https://disc.gsfc.nasa.gov/datasets/M2T1NXLND_5.12.4.
GKU SKPOS®. *SKPOS* [online]. [Accessed May 2023]. Available from: https://www.skpos.gku.sk/en/.
GOODKIND, J. M., 1999. The superconducting gravimeter. *Review of Scientific Instruments*. Online. November 1999. Vol. 70, no. 11, p. 4131–4152. DOI 10.1063/1.1150092.
GPHONEX gravity meter. *Micro-g LaCoste* [online]. 22 October 2020. [Accessed May 2023]. Available from: https://microglacoste.com/product/gphonex-gravimeter/.
Grace - Earth Missions - NASA Jet Propulsion Laboratory. *NASA Jet Propulsion Laboratory (JPL)*. Online. [Accessed 22 May 2023]. Available from: https://www.jpl.nasa.gov/missions/gravity-recovery-and-climate-experiment-grace
HAAGMANS, R., TSAOUSSI, L., MASSOTTI, L., MARCH, G. and DARAS, I., 2020. *Next Generation Gravity Mission as a Mass-change And Geosciences International Constellation (MAGIC) Mission Requirements Document* Online. European Space Agency.
HABEL, B., JANAK, J., PAPCO, J., VALKO, M. 2020. Impact of environmental phenomena on continuous relative gravity measurements performed in urban area. Studia Geophysica et Geodaetica. 64, p. 330–348. DOI 10.1007/s11200-021-0536-4.
HAMMOND, J. and FALLER, J., 1967. 12.5 - Laser-interferometer system for the determination of the acceleration of gravity. IEEE Journal of Quantum Electronics. Online. November 1967. Vol. 3, no. 11, p. 597–602. [Accessed 30 May 2023]. DOI 10.1109/JQE.1967.1074413.
HARTMANN, T. and WENZEL, H. G., 1995. The HW95 tidal potential catalogue. *Geophysical Research Letters*. Online. 15 December 1995. Vol. 22, no. 24, p. 3553–3556. DOI 10.1029/95GL03324.
HEISKANEN, W. A. and MORITZ, H., 1967. Physical Geodesy. W.H. Freeman and Company, San Francisco.